

Flight Deck Aerodynamics of a Nonaviation Ship

M. M. Rhoades* and J. Val. Healey†
Naval Postgraduate School, Monterey, California 93943

The lack of aerodynamic design of ship superstructures has resulted in sharp-edged box-like structures that generate extremely turbulent recirculating flows which wreak havoc with slow moving helicopter blades and place severe and unnecessary limits on naval operations. Furthermore, there is little understanding of the nature of the flows and no data of the flow statistics from locations where such blades operate, which denies the opportunity of analytically studying the problem. It is possible that the very unfavorable airflows around such ships can be controlled by deflectors, vortex generators, etc., but this first requires an understanding of the flow that is to be controlled. This study investigates in considerable detail the nature of the flow patterns over the aft flight deck of a typical nonaviation scale-model ship in a simulated atmospheric boundary layer and made three-dimensional hot-wire measurements of the flow at four points around the locus of a helicopter blade tip for six ship yaw angles. The results will serve as a preliminary data base for the analysis of the blade strike problem and comparison with future computational fluid dynamic (CFD) predictions, in addition to providing a datum from which flow-tailoring can proceed. Extreme levels of velocity gradients and turbulence intensities were found to exist over the flight deck.

I. Introduction

In modern times, the helicopter has become more and more an integral part of shipboard operations, with reconnaissance and logistic support being two of the more standard missions. Ships are broadly divided into two classes: aviation (or carriers) and nonaviation. However, most ships have poor aerodynamic features that render helicopter operations unnecessarily more difficult and hazardous. In construction or retrofits of these nonaviation ships, a boxy sharp-edged hangar, placed immediately forward of the flight deck, is the conventional solution to the problem of helicopter storage.

This nonaviation ship design has been associated with numerous problems over the years, one of which occurs when the helicopter's blades impact on the fuselage of the helicopter while the rotor is turning. This is called a "blade strike," and it typically occurs in the low rotor rpm regime (less than 20% of normal rotor rpm), which is encountered during rotor engagement and disengagement. In an attempt to avoid blade strikes, safe rotor engagement/disengagement envelopes are determined by testing the particular helicopter/ship combination at sea. These "safe" operating envelopes are then used in routine operations thereafter. In addition to the above-mentioned envelopes, landing/takeoff envelopes are also determined by the same process. Determination of these envelopes is called "dynamic interface testing" and is accomplished by testing the various flight operations of the desired type of helicopter on and around the desired ship. This testing determines what wind speed and direction combinations allow safe operation and is a long, laborious, and expensive process; furthermore, it is frequently aborted or curtailed because of calm weather. In addition, it is valid only for the particular ship-helicopter combination tested. Frequently, this type of testing just does not produce a consistently safe envelope because the environment of the open ocean is a poor laboratory and is not cooperative enough to allow thorough, uni-

form testing. Nevertheless, no better method exists, so dynamic interface testing has continued.

Blade strikes can be expensive, even to the extent of the total loss of the helicopter, which underscores the need to investigate their causes. One particular helicopter/ship combination has had a long history of blade strikes, and it is on this combination that the present paper focuses. This study attempts to circumvent the lack of control inherent in nature by using a wind tunnel that is set up specially to simulate the atmospheric boundary layer. This tunnel provides the uniform conditions necessary to determine in detail the flow patterns around the flight deck area. From studying these flow patterns it was hoped that the major contributing factors of the blade strike problem could be identified. Moreover, this ship has a hangar/flight deck combination that is so typical that it can be regarded as almost generic. The results of this study will also provide a datum, from which improvements in the flow quality can be achieved. Such improvements will involve tailoring or controlling the separated flow by using deflectors or other such devices and could widen the safe operating envelopes. A broad review of the dynamic interface problem appears in Ref. 1.

A longer term aim of the dynamic interface community is to simulate helicopter flight in the ship environment. To minimize cost, the wakes should be determined numerically. At the present time, however, potential CFD techniques that can predict the spectra of the velocity fluctuations can be applied only to problems with simple boundaries. It is probable that within 10 years fluctuating velocity spectra prediction in the ship environment will be possible, and this study will assist the validation of such results. At the present time, the mean flow predictions of the time-averaged Navier-Stokes equations could be compared with the mean values of the measurements; however, such predictions would be useless for simulation, because the turbulence spectra are a crucial part of the ship wakes.

In the present study, extensive flow-visualization has been carried out. This was followed by three-dimensional hot-wire measurements at the elevation of the ship's anemometer and at four points around the helicopter blade-tip locus for a range of ship yaw angles. These data should provide a mini-data base for analyzing the blade motion of the helicopter using a suitable mathematical model. A previous attempt at such an analysis of the same blade-strike problem² used measurements

Received Feb. 14, 1991; revision received June 21, 1991; accepted for publication July 28, 1991. This paper is declared a work of the government and is not subjected to copyright protection in the United States.

*Student Member, Department of Aeronautics and Astronautics.

†Associate Professor, Department of Aeronautics and Astronautics.

taken on an oil rig. Such was the lack of data on ship airflows. Until the present paper, no suitable data have been available.

It is not the intention of the present paper to discuss in fine detail the nature of the flows around the flight deck; it is rather to report on the search for possible origins of the blade strikes and on the disastrous consequences of ignoring aerodynamics in the design of ships.

II. Background

A. Modeling the Atmospheric Boundary Layer

The atmosphere to which a real ship is exposed in strong winds is a sheared turbulent boundary layer, a fact that has escaped many researchers. Detailed discussions appear in Refs. 3 and 4. Analysis of the data from the clean tunnel⁴ indicates that the velocity, turbulence intensity, longitudinal length scale, and spectrum function scale up from the model to full size quite well. This was shown by comparing the measured quantities, in suitably nondimensionalized form, with similarly treated measurements that were made in the atmosphere.

B. Bluff-Body Aerodynamics

From the aerodynamic standpoint, a bluff body is one that has, for given flow conditions, a massive separated region in its wake.¹ Even the most modern aviation or nonaviation ships, largely because of the lack of aerodynamic design, must be classified as the worst kind of bluff bodies—ones with sharp edges.

One of the simplest sharp-edged bluff bodies is a cube, of which a classic study was made by Hunt, Abell, Peterka and Woo.⁵ They established the presence of an inverted U-shaped vortex on the downwind side of the body whose ends remained in contact with the ground. In addition, it was established that turbulence causes the re-attachment point to be highly unstable and alters the flowfield around the body by producing increased mixing near the separated shear layers. Moreover, there were "horseshoe" or "necklace" vortices wrapped around the base of the cube that were evident well downstream. Johns and Healey⁶ did a study of the broader features of the flow around a model of a particular ship and found some resemblance between the flow over the flight deck at zero yaw and the wake of a cube.

The airwakes of buildings and ships have much in common, and, since the number of studies of ships is few, much can be learned from building analyses, especially since the ships usually possess the similar cubical or parallelepiped shapes with sharp edges. Typically, the approaching flow is divided by a streamline, that stagnates on the upwind face of the building at about two-thirds of the height. The location of the point is dependent to the first order, on building height-to-width ratio, building height-to-boundary layer height ratio, and upstream surface roughness.⁷ The flow below the stagnation line moves downwards, rolls up into the horseshoe vortices at the

base, and trails downwind. The wind that approaches above the stagnation point flows upwards towards the roof and outwards towards the front vertical edges of the structure. It then separates at these edges and may or may not re-attach to the structure before reaching the leeward edges. This re-attachment depends on many factors, such as building length-to-width ratio, height-to-length ratio, and upstream roughness.

The rear or leeward face of the building is covered by a cavity whose length is defined by the distance from the rear face of the building to the mean reattachment zone on the ground downwind. This distance can vary from two to six building heights (Ref. 21 in Ref. 7). Obtaining a clear picture of the flow in this separation cavity is quite difficult due to the high level of turbulence and the recirculating flow inside this region. Bearing in mind that the size and position of the cavity changes substantially with ship yaw angle and, to some degree, with pitching and rolling of the ship, it is little wonder that creating an accurate rotor engage/disengage envelope has been both difficult and unsuccessful.

III. Experimental Apparatus and Procedure

A. Wind Tunnel and Ship Model

This study was conducted in the Naval Postgraduate School's flow-visualization wind tunnel, which had been modified previously to simulate the atmospheric boundary layer for ship airwake studies.

The tunnel has an open-circuit with air entering an inlet that measures 4.5×4.5 m (15 × 15 ft). The flow first passes through a 75 mm (3 in.) honeycomb, after which a 9:1 ratio square contraction cone directs the flow into the test section of 1.5×1.5 m (5 × 5 ft), and 6.7 m (22 ft) long. The air then exhausts into the atmosphere through a fan with variable pitch blades. A circular turntable which was located in the floor of the tunnel, supported the ship model at the waterline and permitted the necessary rotary motion to reach the yawed positions. Of greatest interest in the present study was the flow over the aft flight deck, with the wind approaching from the port side. The highest frequency of blade strikes occur under these conditions, and the study was confined to this regime. The angular position was measured clockwise from the ship's head, with straight ahead being the 0 deg relative position and directly behind being the 180-deg position; this is the conventional procedure. The position of the ship model was varied through the following yaw angles: 0, 30, 50, 70, 90, and 110 deg. These were all measured clockwise from the tunnel centerline to the ship's longitudinal axis. No pitch or roll effects on the flow around the stationary model were examined in this study because of earlier experience.⁶

B. The Model

A $\frac{1}{16}$ -scale model of the ship, whose hangar/flight deck is shown in many of the figures and labeled as such in Fig. 1,

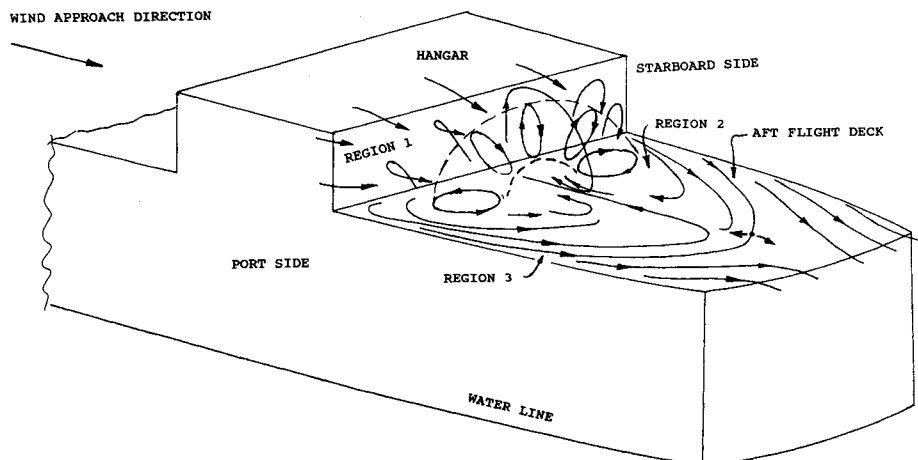


Fig. 1 Flow pattern at 0-deg yaw.

was constructed of wood. To study the flow in the region where most helicopter blade strikes occur, a 47-mm-diam. (1.85 in.) hoop was constructed of 0.79-mm-diam. ($\frac{1}{16}$ -in.) wire and positioned so that it coincided with the locus of the blade tip. The elevation was 30 mm ($\frac{1}{4}$ -in.) above the flight deck, which corresponds to 5.13 m (17.1 ft) full scale. The wire hoop is shown in position in the photographs.

C. Flow Visualization

Visualization was achieved via smoke and helium bubble contamination of the flow. The former was used because of the ease of injecting it through small diameter tubes into the regions of interest. The primary disadvantage of using smoke is that, in highly turbulent flows such as used in this study, the smoke streak lines disperse quickly into an amorphous cloud. However, before this occurs, smoke provides an accurate though limited view of the flow. Unfortunately, it is not possible to obtain clear still photographs because of the dispersion. To overcome this problem, illustrations that were derived mainly from video recordings have been used to show the mean streak line patterns.

The second contaminant used was helium bubbles which are made of a soap/glycerine mixture, filled with helium gas, and made neutrally buoyant by passing them through a centrifugal filter. Unlike the smoke, the bubbles injected into the flow upstream of the model allow clearer visualization of the flow and in much larger regions than is possible with the smoke. However, the greatest disadvantage of using helium bubbles is that they reflect only about five percent of the incident light,⁸ so careful selection and placement of light sources is required.

Capturing a three-dimensional flow field on a two-dimensional photograph appeared and was difficult. It required many long and laborious hours to set-up and trial-and-error to match correctly the lighting, camera position, exposure time, and lens settings required to obtain a good clear picture. The helium bubbles usually scatter and tend to avoid the regions of highest interest, such as recirculation zones; and two methods were employed to overcome this problem: 1) lengthening the exposure times, which allowed more bubble traces to be captured on the photograph and thus increasing the probability that some bubbles would enter the region of interest; and 2) injecting the bubbles as closely as possible to the area of interest without unduly disturbing the flow. Most of the aperture settings were in the region of f5.6 to f16 at about 2 s. A disadvantage of this extended time is that unsteady events of short duration can be missed easily.

Recording of the video was much less demanding than taking the still photographs, with the placement of the lighting being less critical. To deal with the limited view that the single smoke probe provided, an imaginary grid was used to divide the region above the flight deck. The intersections of six vertical and three horizontal planes were utilized as positions for the smoke probe. About thirty smoke tube locations were used for each ship yaw position.

D. Photography and Video Systems

A medium-format camera and fine-grained Kodak T-Max film were used for the still photography. Since the ambient light level was extremely low, Polaroid 3000 ASA film was used to determine the correct exposure. The video equipment was a high-resolution surveillance-type system with a super-VHS video camera recorder.

Several 150- and 300-Watt Xenon arc lamps, all of which had attached collimation optics, were used for the light sources.

E. Hot-Wire Anemometer and Measurements

A commercial hot-wire anemometer was used initially to calibrate the wind tunnel, and the results are presented in Ref. 4. The three-dimensional probe was also a commercial type and was used in conjunction with the necessary bridges, signal conditioners, and an analog/digital (a/d) board, which

had a maximum sampling rate of 50,000 Hz. Calibration of the probe was performed in a commercial unit which had a convenient scan-down feature that reduced the velocity gradually. The unit was also graduated in pitch and yaw, which facilitated reading checks. A detailed discussion of hot-wire anemometry appears in Refs. 9 and 10.

The primary computer for this study was a 25-MHz machine with a 300-MB hard disk and 16 MB of random access memory. The hot-wire data were acquired through the 12 bit a/d board installed in the computer.

Measurements were made at the ship's anemometer position and at four locations around the periphery of the wire hoop when the latter was removed. During the measurement process, the probe pointed up-wind, parallel to the axis of the tunnel, and the ship was rotated to the various yaw positions. By earlier experimentation, it was found that the triple probe could determine the pertinent velocity statistics to within acceptable levels so long as the instantaneous velocity vector remained within 20 deg of the probe axis. The raw voltage signal was passed through the signal conditioner, which incorporated an adjustable low-pass filter set at 1 kHz, and the amplifier was set to a gain of five. After conditioning, the signal was sent to the a/d converter and placed immediately on the hard disk for later processing.

A total of 65,536 measurements per channel was made at a rate of 2 kHz for each of five locations per yaw position. This large number was required to resolve the low-frequency velocity fluctuations that dominated the turbulence; samples of about 8,000 measurements showed considerable variability when taken in succession at the same point. Further measurement details are given in Ref. 4.

IV. Results

To illustrate the various flow patterns, photographs showing the traces of helium bubbles and three-dimensional sketches showing the streak lines, are provided. The patterns shown represent a very rough mean of the flow, which was exceedingly turbulent. There was substantial fluctuation about the streak surfaces shown, with frequent "blobs" of fluid being thrown out. The flow patterns indicated are intended only to give approximate envelopes for the different regions.

Generally, four distinct flow regions exist over the flight deck and all fluctuate to some degree in both size and position:

1) The first is a recirculating zone that is located on the aft face of the hangar inside the port corner. For one yaw angle, this fluctuates almost periodically in size from relatively small to massive. For most yaw angles, the fluctuation was intermittent.

2) The second is a region over the starboard edge of the deck, and it was generally very unsteady. In this region, a backflow from the wake of the ship comes over the edge and inboard, sometimes fluctuating very strongly and extending inboard over most of the deck. It then rises sharply and flows downwind at heights that were very yaw-dependent and often higher than the hangar.

3) The third is a recirculating zone that begins at the windward edge of the deck and extends inboard a distance that varies intermittently with time. This region is relatively low, usually below the hoop elevation, and at some yaw angles, it appears and disappears intermittently.

4) The fourth is the flow external to the above recirculating zones and is generally relatively smoother than that in the other zones.

As the bounding shear layers move about, the levels of turbulence change very rapidly in the zones. For many yaw angles, the large recirculation zones collapse intermittently and re-form.

In many of the yawed positions, introducing the helium bubbles at floor level downwind of the model leads to an uncanny experience. The bubbles rise up the hull, cross over the starboard edge of the deck, and sometimes travel almost

the full width of the deck in the upwind direction. It is a little like watching water flowing uphill.

Interpretive diagrams, drawn from studying the video recordings of the smoke visualization, are given for several of the yaw positions. Space limitation does not permit all positions to be illustrated.

A. 0-Deg Yaw Position

The class of ship studied was very symmetrical, which leads to symmetric flow patterns over the deck as shown in Fig. 1. This flow is similar to that found on the leeward side of the cube in Ref. 5. There is a recirculation region 1 just behind the hangar that is bounded by a shear layer that attaches on the surface of the flight deck. It is clear that there is very little of the deck that is exempt from this recirculation. The velocities and turbulence levels are lower than those found in the other yaw positions. The flow that comes up and over the port and starboard deck edges is more or less smooth, with insignificant recirculating zones just inside the edges. The whole recirculation occasionally appears to collapse partially.

B. 30-Deg Yaw Position

The 30-deg flow pattern is roughly intermediate between the zero and 50-deg yaw positions shown in Figs. 1, 2, and 3. Region 1 of Fig. 1 has been displaced from its symmetric position straddling the ship's axis to the forward starboard corner, where it intermittently collapses and re-forms. Occasionally, it appears like Fig. 2 but is more confined to the forward starboard corner of the deck and less tall, not extending as much above the hangar roof. Helium bubbles were observed, on occasion to cross most of the deck from the lee of the ship at a location just aft of the hangar.

As one goes to higher elevations above the flight deck, approximately 125% of the hangar height, the flow rapidly becomes smoother in the direction of the freestream. Most of the time, much of the ring periphery is exposed to backflow from the lee of the ship.

C. 50-Deg Yaw Position

Figure 2 represents the situation at one extreme: when the recirculation zone 1 has reached its maximum size and approximately three-quarters of the flight deck is engulfed in a very turbulent flow. There is a strong inflow over the starboard edge from the leeward side of the ship that crosses most of the deck, then rises and returns. This could also be interpreted as the disappearance of region 1 and its replacement by a portion of region 2. Of all the yaw angles studied, this position has the largest recirculation zones.

Figure 3 illustrates the flow pattern at the other extreme of the cycle, when the recirculating zones are relatively small. Near the deck, the flow over the recirculating regions 2 and 3 is relatively smooth.

Figure 4 is a photograph taken from a high aspect showing the regions 2 and 4 described earlier. The bubble traces indicate that the external flow is relatively smooth and show a massive and turbulent wake in the lee of the ship. The portion of the hoop to the right appears to be immersed in a smooth,

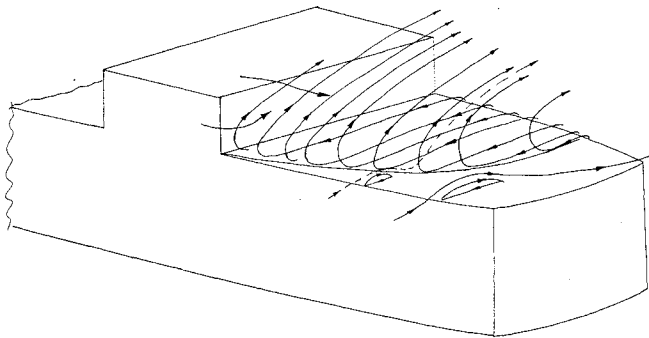


Fig. 2 Flow pattern for one extreme at 50-deg yaw.

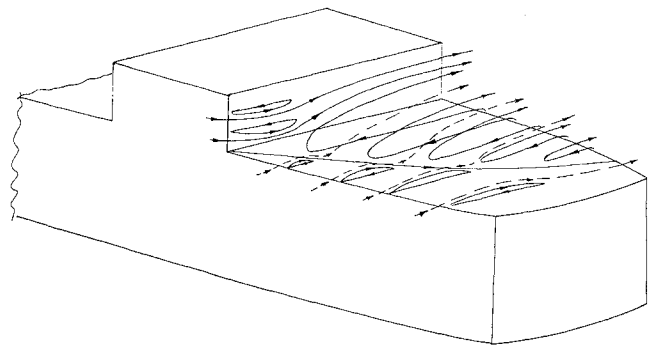


Fig. 3 Flow pattern for other extreme at 50-deg yaw.

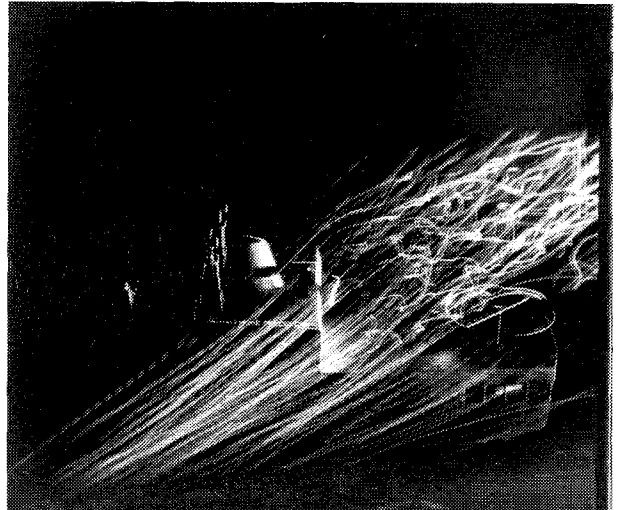


Fig. 4 Bubble streak lines from high aspect at 50-deg yaw.

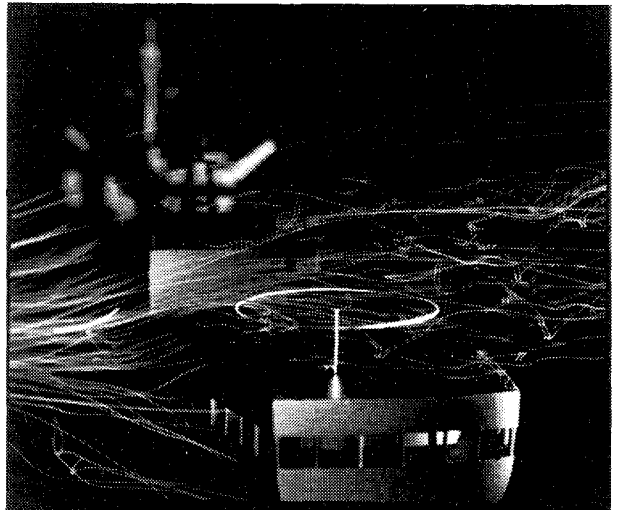


Fig. 5 Bubble streak lines from low aspect at 50-deg yaw.

uniform flow. Quite frequently, the flow in the extreme case shown in Fig. 2 gusts sharply up through the leeward periphery of the hoop. The maximum wake height extends from the deck to an elevation of about 1.5 to 2 times the hangar height, as shown in Fig. 5. Some of the streak lines shown there are due to bubbles returning from the wake.

When visualizing the flow with smoke, a unique feature of this position became evident. It appeared that the aft port hangar corner was shedding vortices when the video of the smoke was viewed at normal recording speeds. When the same recording was viewed in slow motion, it was found that the recirculation, which forms near the aft port corner (region 1), grows in size and that the re-attachment point moves starboard towards a position where it ultimately detaches from

the hangar face. This position is at about 60% of the hangar width from the port corner; and, when the shear layer detaches, the circulation continues, and its center moves downstream and across the deck at an angle about 45 deg to the hangar face plane. In general, in this forward recirculating region 1, there is a counter clockwise motion superimposed on the flow shown. To add that component to the diagram would be difficult. Figure 2 gives the flow when the "vortex" has left the picture and just before the flow switches to that shown in Fig. 3. This happens very quickly, on the order of 1/6 to 4/15 s, based upon the video camera's shutter speed of 1/30 s; it repeats almost periodically. This caused the smoke streak lines to form puffs, and the process appeared to be that of vortex shedding. Strouhal scaling this dynamic process indicates that, on the real ship, the corresponding range is about 2 to 3.3 s. Interestingly, the still photos give no indication that this is happening.

When the shear layer detaches, the forward part of region 2 grows extremely rapidly, with flow crossing most of the deck and rising to an elevation well above that of the hangar before retreating to the lee of the ship again.

As the fan tail is approached, the recirculation zones 2 and 3 become much smaller, giving a fairly smooth flow across the whole deck.

D. 70-Deg Yaw Position

The 70-deg position yielded results, shown in Fig. 6, somewhat similar to those found for the 50-deg position, but the recirculation Region 1 is not as large as is less vigorous. The flow in this region recirculates in an elliptical pattern that had a larger length-to-width ratio than the 50-deg position. This results in smoother conditions over the flight deck generally, especially since region 1 is now mostly forward of the hoop.

Another notable difference is that the shear layer remains attached to the rear hangar face, with the re-attachment point moving port and starboard between about 60 and 80% of the distance across. Recirculating region 2 still expands well onto the deck at one extreme, then retreats back almost to the starboard edge, and oscillates intermittently between the two. Most of the turbulent activity appears to be confined to or below the elevation of the hoop. The extent of the movements of the zone boundaries is shown by the double-dashed lines with the two arrowheads.

E. 90-Deg Yaw Position

It was estimated that the velocity vector over the port edge makes an angle of 15–20 deg with the horizontal. In the relatively benign extreme of the flow in this yaw position, Region 1 has a slightly larger recirculation than that shown in Fig. 3. Region 3 now extends about one-quarter of the way across the deck and is a maximum of about one quarter of the hangar height. Region 2 does not exist now, except for an occasional small burst.

In the other extreme, region 1 has expanded, and the flow detaches from the hangar face. This zone is now similar to that shown in Fig. 2 but is much smaller and confined to the forward one-quarter of the deck. Region 3 now extends all

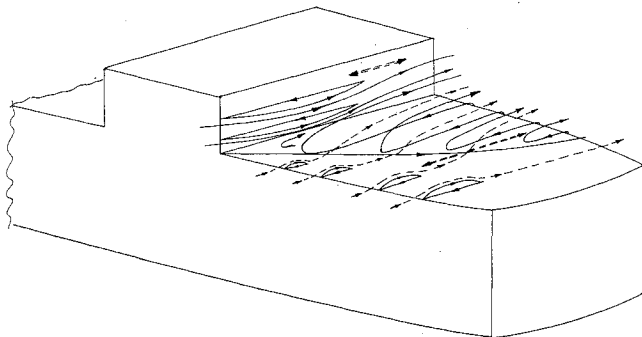


Fig. 6 Flow pattern at 70-deg yaw.

the way across the deck and increases somewhat in height. The flow switches intermittently between these two positions. Figure 7 shows the extremely complex motion of the bubbles whirling around in region 3 and extending up to the hoop level.

F. 110-Deg Yaw Position

Figure 8 illustrates the flow pattern for this case, with the double-dashed lines and two arrow-heads again showing the extent of the movements. This position proved to have the greatest extent of smooth flow over the deck, due largely to the smallest zone 1. Even this zone fluctuated strongly in an intermittent way. This smooth flow is strikingly evident in Fig. 9 by the almost perfectly straight bubble traces. The air

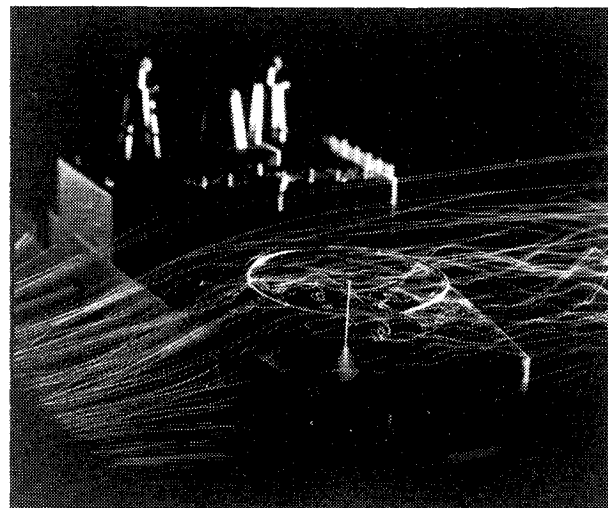


Fig. 7 Bubble streak lines at 90-deg yaw.

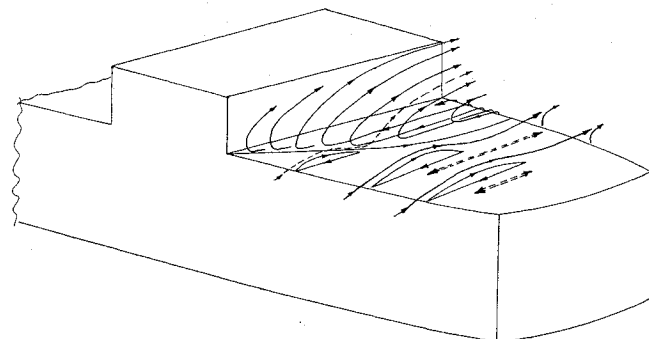


Fig. 8 Flow pattern at 110-deg yaw.

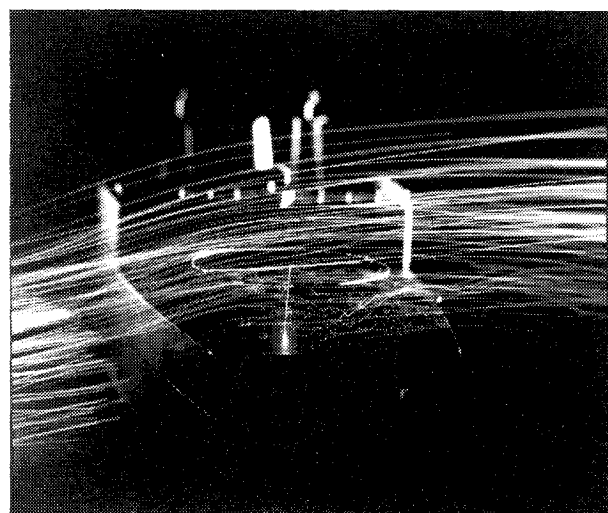


Fig. 9 Bubble streak lines at 110-deg yaw.

coming over the port edge of the deck has a significant upward component; and, like the 90-deg case, the angle was estimated to be approximately 15–20 deg from the horizontal. This upward component is caused by a significant recirculation from region 3 as shown in Fig. 12. Occasionally, a region 2 recirculation appears briefly, and this is shown by the rising bubbles under the starboard side of the hoop.

G. Hot-Wire Anemometer Results

After the measurements were complete, the velocity vector was computed for each point and yaw angle. In all cases, this vector approached the probe within a 20-deg cone around the probe axis. It was previously determined that this was a satisfactory envelope for the range of velocities measured here. The graphs presented are straight-line fits of the data collected at six values of the ship yaw angle. Attempts to smooth the data using low-degree polynomial fits showed too much overshoot due to the rapidly changing values.

The three velocity components are each made nondimensional with the speed or magnitude of the velocity vector at the ship anemometer position.

Figure 10 represents the u components of the velocity at the points 1 through 4 around the blade-tip circle as a function of yaw. As shown on the inset circle, point 1 is forward; 2 is on the starboard (leeward) side; 3 is aft; and 4 is on the port side from which the wind always approaches in this study. The velocities in this and the following diagrams are made nondimensional with the ship anemometer speed for each yaw angle. The maximum value encountered is at point 1 at 70 deg, and this is 110% of the speed. Apart from this point, the velocity components are less than the anemometer speed for all the yaw angles. At zero yaw, the u component at all four points is about 42% of the speed, and, as the yaw angle is increased, the values at points 3 and 4 rise rapidly while 1 and 2 remain "sheltered" by the hangar until the yaw reaches 30 deg. The values at all points reach a maximum of 90 to 110% of the speed. This is followed by a steep decrease to about 70 to 88% at 90 deg and another increase to between 91 and 98% at 110-deg yaw.

From the graph, not shown here because of space limitations, it was evident that the magnitudes of the transverse (v)

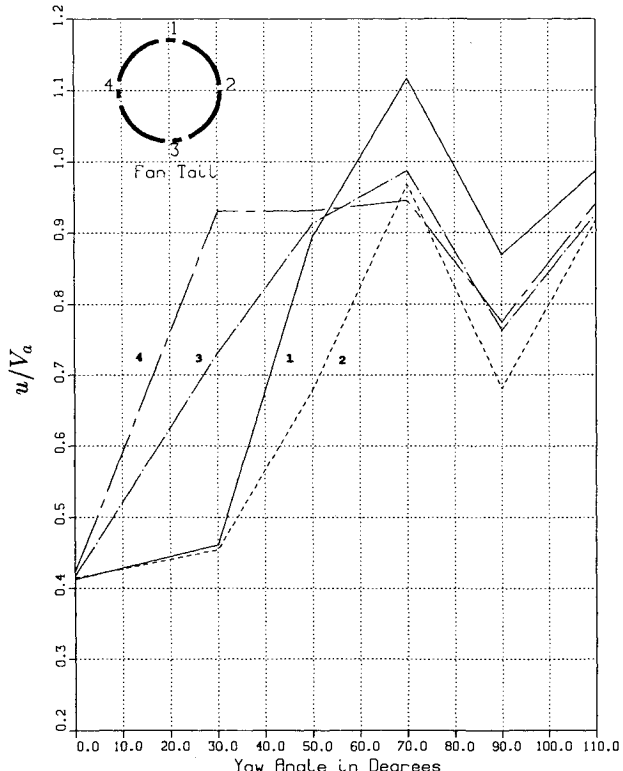


Fig. 10 u/V_a vs yaw angle at points 1 through 4.

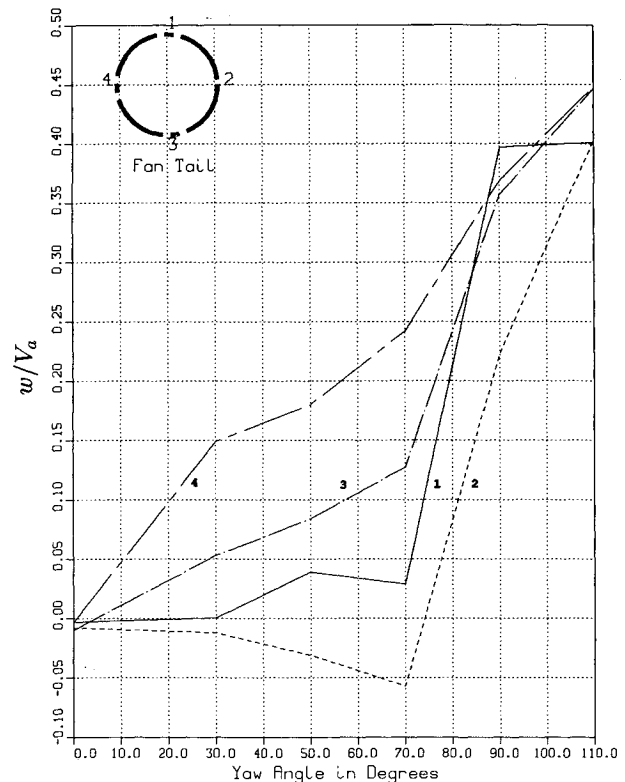


Fig. 11 w/V_a vs yaw angle at points 1 through 4.

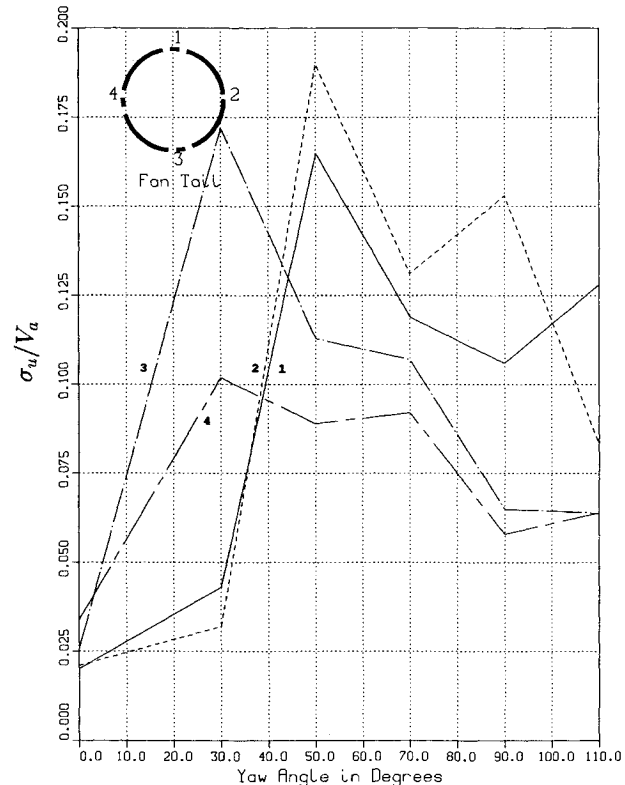


Fig. 12 u Turbulence intensities vs yaw angle at points 1 through 4.

components of the wind velocity are considerably less than the along-wind components. The maximum transverse wind is about 19% of the speed and occurs at point 1 at 110 deg. All velocities start at zero yaw with a slight starboard value. This flow increases until the angle is about 30 deg. In the yaw range of 30 to 60 deg, all values pass through zero, and then the flow to port increases to a maximum at about 70 deg, followed by steep falls to 90 deg. Point 1 shows dramatic

swings from about 12% to port at 70 deg, to about 9% to starboard at 90 deg, and back to about 19% to port at 110 deg. The transverse flow at point 2 varies but little within the band $\pm 4\%$.

The vertical velocities are given in Fig. 11, and they show a much greater variability than the transverse. At all points, there is a very slight downflow at zero yaw. The values at points 3 and 4 rise steeply all the way to 110 deg, while the values at points 1 and 2 vary within a $\pm 5\%$ to 70 deg, followed by dramatic rises to about 40% at 110 deg. At the latter yaw extreme, all values lie within the range 40 to 44% of the speed—remarkably high values.

All the turbulence intensities are formed by dividing the standard deviations of the fluctuations by the ship anemometer speed, in the same manner as the velocities just discussed. This appears to be standard practice in fluid measurements¹¹ in which one of the velocity components is very significant and the other one or two relatively very small. This, however, camouflages the fact that the turbulence intensities formed using the pertinent local component of the velocity become very large—in fact, way beyond what would be considered the normal range of accuracy of hot-wire anemometers.

The along-wind turbulence intensities, as given in Fig. 12, all start about 3% at zero yaw and rise in proportion to the u component of the velocity. At point 3, the value reaches about 17% of the speed and then declines fairly steadily to about 6% at 110-deg yaw. At point 4, the maximum is about 10% at 30 deg, and it declines, also fairly steadily, to the same value as at point 3 at 110 deg. Points 1 and 2 reach their maxima between 16 and 13% at 50 deg and decline sharply to 70 deg. Then the point 2 value rises to about 15% and finally plummets to about 8% at 110 deg; while at point 1, it drops from about 12 to 10.6% between 70 and 90 deg, followed by a rise to about 13%.

The transverse turbulence intensities, which are not shown, indicate that at points 1 and 2, there is a fairly steady rise from about 1.5% at zero yaw to a very significant 18%, approximately, at 110-deg yaw. At point 4, it rises from about 5% to about 9% at 30 deg, levels off roughly to about 70 deg,

and then climbs steadily to about 15% at 110 deg. The value at point 3 rises from about 2% to about 14% at 30 deg, drops to about 10% at 50 deg, levels off to 70 deg, rises to 15% at 90 deg, then drops at 13% to 110 deg.

The vertical turbulence intensities, given in Fig. 13, are on the order of two-thirds the values of those of the u components, with which there is a remarkably strong correlation. The peaks and troughs of both u and w intensities occur at closely the same yaw angles. It is noted that, apart from the 0 to 30-deg yaw range, there is little correlation between the u and w components of the velocities.

V. Conclusions

The air flow over the model ship has four distinct types of regions: three inner ones that are extremely turbulent and dominated by recirculations and an outer one characterized by relatively smooth flow. The boundaries between the regions are shear layers that emanate from the aft edges of the hangar and the port and starboard edges of the deck. The relative sizes of the regions are very dependent on the approach angle of the wind (or the yaw angle of the model).

The highest mean vertical velocity components occur at the 110-deg angle of yaw and the corresponding along-wind and transverse components at about 50–70-deg yaw. The highest along-wind and vertical turbulence intensities occur in the 50–70-deg range, and the corresponding transverse component at 110-deg yaw.

If turbulence intensities are formed with the local values of the mean velocities, all measurements had values in excess of the usual 30% of at least one of the velocity components, and many of the histograms of the velocity fluctuations were grossly distorted and asymmetric. This casts doubt on the accuracy of hot-wire anemometer measurements, especially near the deck.

The most detrimental aerodynamic features of this class of ship are undoubtedly the boxy sharp-cornered hangar and the adjacent high flight deck. The hangar caused massive recirculations over the flight deck in every case, except the 110-deg angle of yaw, which lends credibility to the suggestion of putting helicopter flight decks forward of the ship's superstructure. However, it is known that many pilots feel very uncomfortable with a massive hangar face coming towards them while they are maneuvering to land.

At ship yaw angles of about 50 deg or less, the forward portion of the rotor blade periphery is subject to the flapping of the shear layers emanating from the aft edges of the hangar and the accompanying strong reverse circulation from the lee of the ship. For greater yaw angles, this flapping layer does not directly envelop the rotor, but the blade trajectory is affected both by recirculating flow from the lee, and another that starts at the port edge of the deck. Both wax and wane in an intermittent way.

The high flight deck causes a considerable blockage to the air flow approaching the side of the ship. The airflow is forced to rise over the flight deck which leads to a significant upward component of flow as the air passes over that edge. If the deck were closer to the water, the flow would not have to rise so sharply and would form a smaller recirculation zone. It is probable that rounding or chamfering of the edge of the deck or the use of deflectors would reduce this problem.

This project started with the hope of identifying a region, or a small number of regions, of particularly adverse flow that might cause the blade strikes. Fortunately, there appears to be little reason for strikes to occur on the aftmost 25% of the blade trajectory. Otherwise in terms of reasonably steady velocities, low velocity gradients, and turbulent levels, the flow quality is very unfavorable.

In an effort to identify local airflows that might cause the strikes, information was requested from various sources within the Navy about the blade motion immediately preceding a

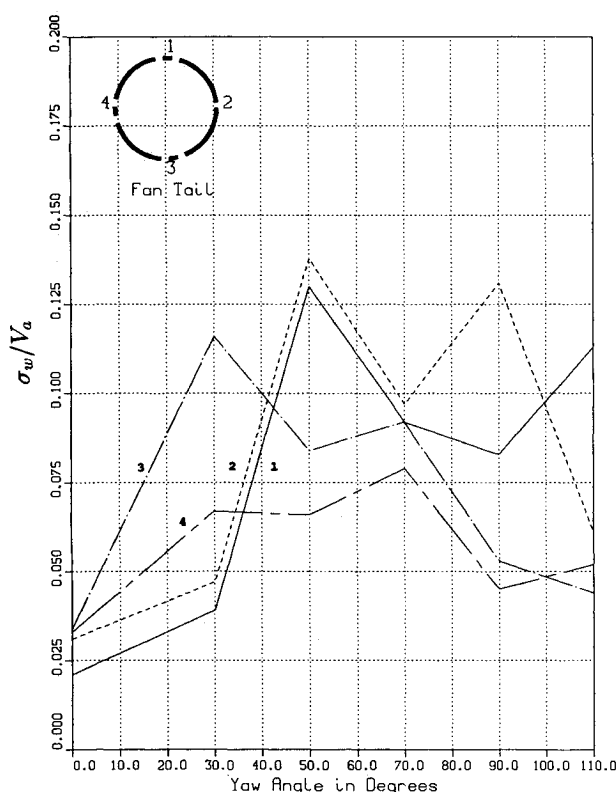


Fig. 13 w Turbulence intensities vs yaw angle at points 1 through 4.

strike. The hope was that the cause could be attributed to the upflow near the edge of the deck or to the strong turbulent eddies in the recirculation zone and that appropriate measures could then be taken to control that particular flow. Unfortunately, the required information was not available.

The only hope of alleviating the blade strike problem on existing ships is to attempt to control the flow, with the view of eliminating some of the more unruly flow patterns, for example, with deflectors or wind breaks or some combination of both. In view of the large number of ships with this hangar/landing deck configuration that will be around for twenty years or more, it is essential that such tailoring be pursued with the aim of widening the operating envelopes and eliminating the blade strikes. This can be done both numerically, using computational fluid dynamics, and experimentally, using reduced and full-scale testing. The results should lead to a greatly increased efficiency in ship/helicopter interactions.

Some other recommendations are:

1) The very low velocities and extreme levels of turbulence make essential the re-taking of data near the flight deck area of the model ship using a pulsed-wire or flying-wire anemometer or possibly a laser Doppler velocimeter. What a turbulence intensity of 100% or more means is extremely uncertain.

2) The effects of the helicopter's fuselage on the flowfield should be investigated, paying particular attention to the local Reynolds number effect on the modeling.

3) Information derived from this study should be compared with the predictions of computational fluid dynamics programs.

4) A detailed study should be made of the air wake of oscillating ship models.

5) The results of this and previous studies indicate that the typical hangar/flight deck combinations are intrinsically aerodynamically unfavorable to rotorcraft operations. It is essential that this message be heeded in the design of new ships. It is very likely that aerodynamically designed ships will have little restrictions on the operating envelopes of rotorcraft and will require little, if any, interface testing. Such a ship would also represent a substantial increase in the efficiency of naval operations and save vast amounts of money on the testing.

Acknowledgments

The authors are indebted to: Jonah Ottensoser and Bob Bailey of the Naval Air Systems Command (AIR 530) and the Naval Postgraduate School for supporting this work; Pat Hickey, Ron Ramaker, and John Moulton for workshop support; The W. R. Church Computer Center at NPS for the use of graphics facilities; Tony Cricelli for his assistance in resolving never ending computer difficulties; M. S. Chandra, NASA Ames Research Center, Moffett Field, CA, for a helpful discussion on hot wire anemometry; and Toni and Christian Rhoades for their patience and understanding.

References

- ¹Healey, J. V., "The Prospects for Simulating the Helicopter/Ship Interface," *Naval Engineer's Journal*, Vol. 99, No. 2, 1967, pp. 45-63.
- ²Leone, P. F., "Analytic Correlation with Mishap Report of a CH-46D Aft Rotor Blade Tunnel Strike Induced by a Wind Flow up through the Aft Rotor Disk During a Startup Operation while Shipboard at Sea, Boeing Vertol Company," IOM 8-7450-PFL-06, April 21, 1982.
- ³Plate, E. J., *Engineering Meteorology*, Elsevier, New York/Amsterdam, 1982, pp. 573-636.
- ⁴Healey, J. V., "Establishing a Database for Flight in the Wakes of Structures," *Journal of Aircraft*, Vol. 29, No. 4, 1992, pp. 559-564.
- ⁵Hunt, J. C. R., Abell, C. J., Peterka, J. A., and Woo, H. "Kinematic Studies of the Flows Around Free or Surface-Mounted Obstacles: Applying Topology to Flow Visualization," *Journal of Fluid Mechanics*, Vol. 86, 1978, pp. 179-200.
- ⁶Johns, M. K., and Healey, J. V., "The Airwake of a DD-963 Class Destroyer," *Naval Engineer's Journal*, Vol. 101, No. 3, 1989, pp. 36-42.
- ⁷Beranek, W. J., "General Rules for Determination of Wind Environment," *Proceedings of the 5th International Conference on Wind Engineering*, Fort Collins, CO, July 1979.
- ⁸Goldstein, R. J., *Fluid Mechanics Measurement*, Hemisphere, New York, 1983.
- ⁹Lomas, C. G., *Fundamentals of Hot Wire Anemometry*, Cambridge University Press, New York, 1986.
- ¹⁰Perry, A. E., *Hot-Wire Anemometry*, Oxford University Press, Oxford, England, 1982.
- ¹¹Chandra, M. S., Private communication, Nov. 1990.